

**PRODUCT VIBRATIONAL ANALYSIS OF ION–MOLECULE REACTIONS
BY LASER-INDUCED FLUORESCENCE IN A FLOWING AFTERGLOW:**



Charles L. HAMILTON, Michael A. DUNCAN^{*}, Timothy S. ZWIER^{**}, James C. WEISSHAAR[‡],
G. Barney ELLISON[‡], Veronica M. BIERBAUM and Stephen R. LEONE[☆]

*Joint Institute for Laboratory Astrophysics, National Bureau of Standards and University of Colorado
and Department of Chemistry, University of Colorado, Boulder, Colorado 80309, USA*

Received 12 October 1982

Laser-induced fluorescence is coupled to a flowing afterglow to obtain product state distributions of thermal energy ion–molecule reactions. For OH produced in the $\text{O}^- + \text{HF} \rightarrow \text{OH}(v=0,1) + \text{F}^-$ reaction, $v=0/v=1$ is 1.0/0.22. Ion vibrational relaxation and obscuring Penning ionization reactions preclude accurate measurements for the $\text{N}^+ + \text{CO} \rightarrow \text{CO}^+(v=0,1,2) + \text{N}$ system.

1. Introduction

Laser-induced fluorescence (LIF) has been applied in many laboratories to study the spectroscopy of ions [1–7], their reaction dynamics [8,9], and deactivation [2,8,9]. However, only in a few experiments have estimates of cross sections or product state distributions been made [3,8–10]. Optical probing of product vibrational states may provide additional insights into the dynamics of ion–molecule reactions which are not obtained by molecular beam scattering techniques [11]. In this paper we report one of the first LIF measurements of a vibrational product state distribution for an ion–molecule reaction. The LIF technique is coupled to a flowing afterglow apparatus, which provides a well-characterized medium for quantitative studies of state distributions and other kinetic and dynamic parameters [12,13].

Two reactions are investigated that demonstrate both the strengths and weaknesses of the flowing afterglow technique. In the proton transfer reaction, $\text{O}^- + \text{HF} \rightarrow \text{OH}(v=0,1) + \text{F}^-$, the $v=0$ and $v=1$ populations are determined by LIF probing of lines in the (1,0) and (1,1) bands of the $\text{A}^2\Sigma^+ - \text{X}^2\Pi_{3/2}$ transition. An attempt is made to obtain the product vibrational distribution in the $\text{N}^+ + \text{CO} \rightarrow \text{CO}^+(v=0,1,2) + \text{N}$ charge transfer reaction by probing the $\text{A}^2\Pi_t - \text{X}^2\Sigma^+$ band of CO^+ . This attempt is frustrated by rapid vibrational relaxation of the nascent $\text{CO}^+(v)$ with both CO and N_2 and by the Penning ionization of CO by residual He metastables. A qualitative estimate of the vibrational relaxation rates of $\text{CO}^+(v=1)$ is obtained, but accurate product state information for the ion reaction cannot be determined.

2. Experimental

The previously described flowing afterglow apparatus [13–16] is modified here to incorporate laser-induced fluorescence detection (fig. 1). The instrument consists of a 7.3 cm diameter flow tube with an electron impact ion source at the upstream end, a quadrupole mass filter to sample the ions through an orifice at the down-

^{*} NRC–NBS postdoctoral fellow.

^{**} Present address: The James Franck Institute, University of Chicago, Chicago, Illinois 60637, USA.

[‡] Present address: Department of Chemistry, University of Wisconsin, Madison, Wisconsin 53706, USA

[†] Alfred P. Sloan fellow.

[☆] Staff member, Quantum Physics Division, National Bureau of Standards.

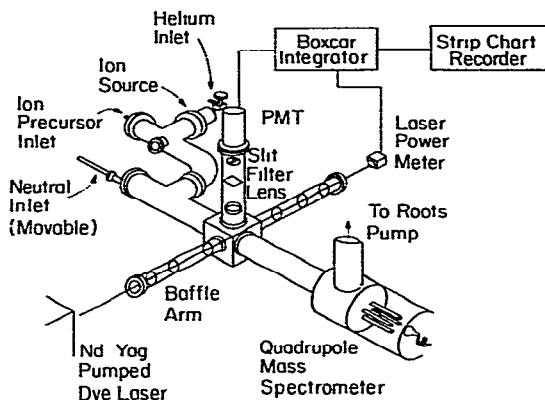


Fig. 1. Flowing afterglow-laser-induced fluorescence apparatus

stream end, a 500 l s^{-1} blower to establish the high-velocity flow of helium buffer gas, baffle arms to introduce the pulsed laser beam, a photomultiplier and its associated fluorescence collection optics, and gated analog signal detection electronics. Fluorescence emitted at right angles to the laser is imaged with a 5.1 cm diameter $f/1$ suprasil lens onto the slit in front of the photomultiplier. The analog signal from the photomultiplier is processed with a boxcar integrator which is gated on just after any scattered laser light and remains on for several μs . The analog output of the boxcar is digitized and also plotted on a strip chart recorder.

The tunable laser source is a pulsed, Nd : YAG pumped dye laser system (5 ns pulses, 10 Hz, 1 cm^{-1} linewidth). Amplified spontaneous emission is suppressed to less than 5% of the narrow line power. Frequency doubling for the OH experiments is accomplished with an auto-tracking, angle-tuned KD^*P crystal. For unsaturated excitation of CO^+ and OH, an energy density of $\approx 0.1 \text{ mJ cm}^{-2}$ is used. The fluorescence signal is normalized to the average laser power, which is measured with a thermopile and monitored with a second channel in the boxcar integrator.

Several modifications are made to reduce stray and scattered light from reaching the photomultiplier. All surfaces within the flow tube are blackened with flat black coating. Stray light from the ion source filament is reduced by incorporation of a 90° elbow between the ion source and the laser detection zone. Scattered laser light is reduced with narrow-bandpass or long-wavelength cutoff filters. A major source of light noise is the gaseous afterglow itself. The ion source generates copious quan-

ties of excited He metastables, which are typically quenched before the reaction zone, but produce emissions upon quenching that reach the photomultiplier. The slit and focusing lens in front of the photomultiplier discriminate the signal photons from this background by a factor of 30. The maximum achievable sensitivity inherent in LIF detection is not observed in these experiments because of the trade-offs between maximizing ion production and minimizing product molecule relaxation and afterglow stray light.

Under some conditions, residual He metastables can produce interfering reactions, such as Penning ionization of CO which obscures the CO^+ from the desired $\text{N}^+ + \text{CO}$ reaction. Similarly, interference from OH produced by impurity reactions in the ion source region can obscure OH formed in the desired $\text{O}^- + \text{HF}$ reaction. Measurement of background signals from either of these sources is accomplished by stopping the ions just prior to reagent addition. A 30 V potential applied to a series of six 1 cm long electrically insulated rings which make up a section of the flow tube stops $\approx 99\%$ of the ions and allows an "ion-on"/"ion-off" measurement of the LIF.

The N^+ ions for the reaction with CO are produced by flowing pure helium over the filament and adding N_2 immediately downstream of the ion source. At N_2 pressures of 0.006 Pa or 0.08 Pa ($1 \text{ Pa} = 7.5 \times 10^{-3} \text{ Torr}$) and helium pressures of 70 Pa, the N^+/N_2^+ ratio is $\approx 20/1$. N_2^+ can also react with CO, and thus must be minimized. The O^- for reaction with HF is produced by passing a mixture of 3.3 Pa of O_2 and 70 Pa of He directly over the filament. Typical reactant ion densities at the laser detection zone are 10^7 cm^{-3} . Neutral reactants, CO or HF (99.9%), are added through a movable inlet at approximate pressures of 0.006 Pa and 0.7 Pa or less, respectively. HF is used directly from the cylinder. He, N_2 and CO are passed through molecular sieve traps, cooled to either 77 K (He) or 195 K (N_2 and CO).

3. Results and discussion

The first reaction studied is the $\text{N}^+ + \text{CO} \rightarrow \text{CO}^+(v=0,1,2) + \text{N}$ charge transfer reaction ($\Delta H = -0.52 \text{ eV}$, $k_1 = 5 \times 10^{-10} \text{ cm}^3 \text{ molecule}^{-1} \text{ s}^{-1}$ [17]). Energy resonance favors population of $v=2$, but the Franck-Condon factors [18] favor population of $v=$

0. CO^+ is observed both by LIF and at the mass spectrometer upon addition of CO to the helium flow containing N^+ . However, experiments in which the ions are stopped by a retarding potential on the rings demonstrate that much of the CO^+ is formed by Penning ionization of CO with He metastables when the pressure of N_2 is below 0.1 Pa. The Penning ionization reaction produces substantial excitation of both CO^+ A and B states [19], which in turn will radiatively cascade to various vibrational levels of the X state. Thus although CO^+ is detected by LIF in both $v'' = 0$ and $v'' = 1$, it is not possible to rule out the production of CO^+ by He metastables under the conditions in which $v'' = 1$ is observed. At higher N_2 pressures where He metastables are completely quenched, rapid vibrational relaxation of $\text{CO}^+(v = 1)$ by N_2 precludes detection of $\text{CO}^+(v = 1)$ within the signal-to-noise.

Attempts to quantify the vibrational relaxation of $\text{CO}^+(v = 1)$ by CO and N_2 are also frustrated by the possible reformation of excited CO^+ in the detection zone by He metastables. Thus it is only possible to conclude that the relaxation rates of $\text{CO}^+(v = 1)$ by CO and N_2 both are rapid, somewhere in the range of 0.1–1.0 of the Langevin rate. Smith and Futrell [20] showed that the $\text{CO}^+ + \text{CO}$ charge exchange has a rate coefficient of $8.5 \times 10^{-10} \text{ cm}^3 \text{ molecule}^{-1} \text{ s}^{-1}$, essentially the Langevin rate. Thus it is likely that the vibrational deactivation of CO^+ by CO proceeds with a rate of at least half that value assuming that the vibrational energy remains with the ion in half of the collisions. For CO^+ deactivated by N_2 , such a resonant charge transfer channel is not open, and the vibrational deactivation, which is also observed here to be extremely efficient, must occur by near-resonant vibration-to-vibration energy transfer.

Because of the difficulties inherent in the charge transfer reaction described above, the second system investigated is the proton abstraction reaction,



($\Delta H = -0.46 \text{ eV}$ (-3710 cm^{-1}) [21–23], k_2 (estimated in this work) $\approx 5 \times 10^{-10} \text{ cm}^3 \text{ molecule}^{-1} \text{ s}^{-1}$). The $v = 1$ state lies 3570 cm^{-1} above $v = 0$. In the reaction of $\text{O}^- + \text{HF}$, in contrast to that of $\text{N}^+ + \text{CO}$, interaction of He metastables with the neutral reagent cannot generate the detected diatomic product; moreover, vibrational deactivation of OH is slower than for an ionic species. However, background levels of OH are produced

in the ion source. The residual $\text{OH}(v = 0)$ is found to be 10–20% of the $\text{OH}(v = 0)$ produced by the ion reaction. This value is the same when either the O^- or HF is stopped. The reported background values are obtained by turning the HF flow off.

Detection is accomplished by probing specifically the $\text{P}_1(2)$ and $\text{P}_1(5)$ lines ($\Delta N = -1$, $\Delta J = -1$) of the (1,0) and (1,1) bands (v', v'') of the OH ($\text{A}^2\Sigma^+ - \text{X}^2\Pi_{3/2}$) transition. A spectrum of the (1,0) band system and those specific lines are shown in fig. 2. The (1,1) band is similar and occurs in the 314 nm region. These lines are chosen because they are well isolated in both bands. Since the same upper state levels are excited in both bands, it is not necessary to correct the signals for photomultiplier response, transmission of the optics, and vibrational deactivation. The rotational line intensities fit a Boltzmann distribution at 300 K, indicating complete thermalization of the rotational levels by the 500–1000 collisions with helium during the time between formation and detection of OH. Line areas are measured with a very slow scan of the laser to obtain the most precise, reproducible results.

The data are reduced in the following way. The signals are normalized for laser power by the dual channel boxcar. The line areas from each run are corrected for the residual OH background, and the signals are normalized for the differences in absorption strengths. The electronic transition dipole moment for the OH(A–X) system is a strong function of internuclear distance. As a result, the band intensities are not simply proportional to the Franck–Condon factors. Various

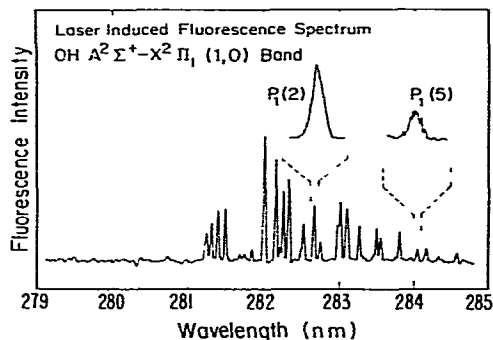


Fig. 2. Laser-induced fluorescence spectrum of the (1,0) band of the OH(A–X) system. The $\text{P}_1(2)$ and $\text{P}_1(5)$ lines are used to determine the vibrational distribution in OH.

Table 1
Signal areas for one set of experiments on the $O^- + HF \rightarrow OH + F^-$ reaction ^{a)}

(1,0) signal ^{b)}	(1,0) background	(1,1) signal ^{c)}
1601	499	763
1660	429	792
1570	475	823
1686	290	771
ave = 1629 ± 53	ave = 312 ± 93	ave = 787 ± 27

- a) Inlet position 2 cm upstream of the LIF region, HF pressure 0.13 Pa, $P_1(2)$ line.
 b) Areas uncorrected for background (arbitrary units) Errors are $\pm 2\sigma$.
 c) No background observed for $v'' = 1$ in any of the experiments reported here or in table 2.

methods for calculating the transition probabilities have been discussed [23], and values have been tabulated for the (0,0), (1,1) and (1,0) bands [24]. The ratios used here for (1,0)/(1,1) are 0.416 for the $P_1(2)$ line and 0.417 for the $P_1(5)$ line. Since the Boltzmann weightings, $e^{-f/kT}/Q$, are slightly different for the $v'' = 0$ and $v'' = 1$ states, the LIF signals are normalized to

them (f is the rotational energy of the N'', J'' state and Q is the rotational partition function). Those ratios for $v'' = 0/v'' = 1$ are 1.019 for the $P_1(2)$ line and 0.942 for the $P_1(5)$ line. Correction for the rotational degeneracy is not necessary since the same lines are compared in each case. The dye laser is scanned in constant wavelength increments per unit time ($d\lambda/dt$), but the formulation of the line area and absorption strength assumes constant frequency intervals. Since $dv/dt \propto -d\lambda/\lambda^2 dt$, the peak areas must be normalized by dividing by λ^2 (a value of 0.809 for the (1,0)/(1,1) ratio).

The $OH(v = 1/v = 0)$ population ratio is measured for HF pressures ranging from 0.13 to 0.93 Pa and for movable inlet distances from 2 to 14 cm upstream of the laser beam. Table 1 shows a representative set of raw data for four runs at one inlet distance and pressure of HF, along with the residual OH corrections. Table 2 displays the final $OH(v = 1/v = 0)$ ratios. Vibrational relaxation of $OH(v = 1)$ by HF is not observed and relaxation by O_2 also appears to be slow. The reduction in the $v = 1/v = 0$ ratio with increasing reaction distance is probably due to relaxation of $v = 1$ at the walls. Extrapolation of the results in table 2 to the shortest reaction distances leads to the final quoted distribution for $v = 0 : v = 1$ of 1.00 : 0.22 ± 0.02. The error represents 95% confidence limits.

Table 2
Final population ratios for $OH(v = 1)/(v = 0)$ from the $O^- + HF \rightarrow OH + F^-$ reaction

Line	Number of experiments	HF pressure (PA)	Inlet distance (cm)	$(v = 1)/(v = 0)$ ^{a)}
$P_1(2)$	6	0.13	2	0.230 ± 0.015
$P_1(2)$	6	0.27	2	0.225 ± 0.017
$P_1(2)$	6	0.40	2	0.235 ± 0.017
$P_1(2)$	6	0.67	2	0.215 ± 0.033
$P_1(2)$	6	0.93	2	0.219 ± 0.021
$P_1(2)$ ^{b)}	4	0.13	2	0.224 ± 0.034
$P_1(2)$	4	0.13	6	0.220 ± 0.024
$P_1(2)$	4	0.13	10	0.193 ± 0.034
$P_1(2)$	4	0.13	14	0.134 ± 0.028
$P_1(5)$	6	0.13	2	0.249 ± 0.029
$P_1(5)$	6	0.13	6	0.200 ± 0.033
final ratio				0.22 ± 0.02

a) Errors reported to 95% confidence based on standard deviations in raw data. There may be some uncertainty in the absorption coefficients; however, this is not included in the error limits.

b) The result from the raw data shown in table 1.

It should be noted that the $P_1(2)$ and $P_1(5)$ lines both sample the $X^2\Pi_{3/2}$ state. The $O^- 2P_{1/2}$, $2P_{3/2}$ states are split by 22 meV [22]. In a separate experiment on the (0,0) band the strengths of the $R_2(N)$ lines ($2\Pi_{1/2}$, $N = 3,4$) are compared to the $R_1(N) + R_{21}(N)$ blended lines ($2\Pi_{3/2}$, $N = 3,4$). The intensities of these lines are completely consistent with a statistical $2\Pi_{1/2}$, $2\Pi_{3/2}$ distribution. Collisional equilibration of the $2\Pi_{1/2}$ and $2\Pi_{3/2}$ states ($\Delta E = 16$ meV [25]) might be expected to be rapid with the helium buffer gas, so it is unlikely that any preferential population of the $2\Pi_{1/2}$ or $2\Pi_{3/2}$ states can be observed here.

The low $OH(v = 1)$ population is characteristic of product states whose energies are close to the reaction exoergicity (the energy in excess of $v = 1$ is 140 cm^{-1}). Earlier experiments on proton abstraction reactions of $C^+ + HBr$, HI [14] and $F^- + HCl$, HBr , and HI [15] showed that the fraction of energy deposited into vibrational excitation is substantial when more energy is available ($f_v \approx 0.3 - 0.5$). In the $O^- + HF$ reaction, there is still a strong propensity to deposit energy into vibration. This is evidenced by the observed 0.18 fraction in $v = 1$ compared to a value of 0.07 calculated for a statistical "prior" distribution [24]. All of the proton abstraction reactions investigated thus far have vibrational product distributions very similar to those of analogous neutral hydrogen abstraction reactions. The neutral analog of the $O^- + HF$ reaction, however, is highly endothermic. The potential surfaces for ion-molecule reactions differ substantially from their neutral counterparts in that the ion reactions have strong, long-range attractive forces, there are often no barriers, and in the case of $O^- + HF$, multiple surface crossings may be important. It remains to be determined by further theoretical analysis how these features of the potential energy surface will affect energy disposal and selectivity in ion-molecule reactions [26,27].

4 Conclusion

We have demonstrated that the flowing afterglow-LIF technique can be used to determine precise vibrational distributions for ion-molecule reactions carried out under well-characterized conditions. The technique also shows excellent promise for measuring the rates of vibrational relaxation and vibration-to-vibration energy transfer in ion-molecule collisions. The present limita-

tions of afterglow emission, unwanted vibrational deactivation, and obscuring reactions may be solved by more sophisticated methods of ion production, such as the mass selected ion introduction technique [28], which eliminates the helium metastables and neutral precursor molecules from the flow tube. Under such conditions, the ultimate sensitivity of the LIF technique is expected to be achieved.

Acknowledgement

The authors are grateful to the Air Force Office of Scientific Research and the National Science Foundation for generous support of this research. CEH wishes to thank the National Science Foundation for a predoctoral fellowship.

References

- [1] P.C. Engelking and A.L. Smith, *Chem. Phys. Letters* 36 (1975) 21.
- [2] T.A. Miller and V.F. Bondybey, *Chem. Phys. Letters* 50 (1977) 275.
- [3] T.A. Miller and V.F. Bondybey, *J. Chem. Phys. Phys. Chem. Biol.* 77 (1980) 695.
- [4] I.J. Grieman, B.H. Mahan and A. O'Keefe, *J. Chem. Phys.* 72 (1980) 4246.
- [5] J. Danon, G. Mauclaire, T.R. Govers and R. Marx, *J. Chem. Phys.* 76 (1982) 1255.
- [6] M. Heaven, T.A. Miller and V.F. Bondybey, *J. Chem. Phys.* 76 (1982) 3831.
- [7] A. Ding, K. Richter and M. Menzinger, *Chem. Phys. Letters* 77 (1981) 523.
- [8] B.H. Mahan, C. Martner and A. O'Keefe, *J. Chem. Phys.* 76 (1982) 4433.
- [9] J. Danon and R. Marx, *Chem. Phys.* 68 (1982) 255.
- [10] J. Allison, T. Kondow and R.N. Zare, *Chem. Phys. Letters* 64 (1979) 202.
- [11] T.O. Tiernan and C. Lifshitz, *Advan. Chem. Phys.* 45 (1981) 81.
- [12] E.L. Ferguson, F.C. Fehsenfeld, and A.L. Schmeltekopf, *Advan. At. Mol. Phys.* 5 (1969) 1.
- [13] V.M. Bierbaum, G.B. Ellison and S.R. Leone, in: *Ions and light, gas phase ion chemistry*, Vol. 3, ed. M.T. Bowers (Academic Press, New York, 1983).
- [14] T.S. Zwier, V.M. Bierbaum, G.B. Ellison and S.R. Leone, *J. Chem. Phys.* 72 (1980) 5426.
- [15] J.C. Weisshaar, T.S. Zwier and S.R. Leone, *J. Chem. Phys.* 75 (1981) 4873.
- [16] M.M. Maricq, M.A. Smith, C.J.S.M. Simpson and G.B. Ellison, *J. Chem. Phys.* 74 (1981) 6154.

- [17] F.C. Fehsenfeld, A.L. Schmeltekopf and E.E. Ferguson, *J. Chem. Phys.* 46 (1967) 2019.
- [18] P.H. Krupenie, *The Band Spectrum of Carbon Monoxide*, NSRDS-NBS 5 (National Bureau of Standards, Washington, 1966).
- [19] P.J. Marcoux, M. van Swaay and D.W. Setser, *J. Phys. Chem.* 83 (1979) 3168, and references therein.
- [20] D.L. Smith and J.H. Futrell, *J. Chem. Phys.* 59 (1973) 463.
- [21] K.P. Huber and G. Herzberg, *Molecular spectra and molecular structure*, Vol. 4. Constants of diatomic molecules (Van Nostrand, Princeton, 1979).
- [22] H. Hotop and W.C. Lineberger, *J. Phys. Chem. Ref. Data* 4 (1975) 539.
- [23] G.H. Dicke and H.M. Crosswhite, *J. Quant. Spectry. Radiative Transfer* 2 (1962) 97.
- [24] R.B. Bernstein and P.D. Levine, *Advan. At. Mol. Phys.* 11 (1975) 215.
- [25] K.M. Evenson, J.S. Wells and H.E. Radford, *Phys. Rev. Letters* 25 (1970) 199.
- [26] S. Chapman, *Chem. Phys. Letters* 80 (1981) 275.
- [27] P. Kuntz, in: *Dynamics of molecular collisions*, Part B, ed. W.H. Miller (Plenum Press, New York, 1976) p. 53.
- [28] N.G. Adams and D. Smith, *Intern. J. Mass Spectrom. Ion Phys.* 21 (1976) 349.